

Direct evidence for a gapless Z_2 spin liquid by frustrating Néel antiferromagnetism

Wen-Jun Hu,¹ Federico Becca,¹ Alberto Parola,² and Sandro Sorella¹

¹ *Democritos Simulation Center CNR-IOM Istituto Officina dei Materiali and*

International School for Advanced Studies (SISSA), Via Bonomea 265, 34136 Trieste, Italy

² *Dipartimento di Scienza e Alta Tecnologia, Università dell'Insubria, Via Valleggio 11, I-22100 Como, Italy*

(Dated: April 10, 2013)

By direct calculations of the spin gap in the frustrated Heisenberg model on the square lattice, with nearest- (J_1) and next-nearest-neighbor (J_2) super-exchange couplings, we provide a solid evidence that the spin-liquid phase in the frustrated regime $0.45 \lesssim J_2/J_1 \lesssim 0.6$ is gapless. Our numerical method is based on a variational wave function that is *systematically* improved by the application of few Lanczos steps and allows us to obtain reliable extrapolations in the thermodynamic limit. The peculiar nature of the non-magnetic state is unveiled by the existence of $S = 1$ gapless excitations at $k = (\pi, 0)$ and $(0, \pi)$. The magnetic transition can be described and interpreted by a variational state that is built from Abrikosov fermions having a Z_2 gauge structure and four Dirac points in the spinon spectrum.

PACS numbers:

Introduction – During the “Valence-Bond-Solid era” most of the community working on highly-frustrated magnets believed that quantum spin liquids could not exist as true ground states of microscopic models and some kind of valence-bond order would have taken place in non-magnetic insulators (thus leading to trivial band insulators). Now, we are presently living the more exciting “Quantum-Spin-Liquid era”, where a plethora of different spin-liquid states are proposed as ground states of various magnetic systems, both theoretically and experimentally.¹ The turning point was marked by the discovery that stable gapped spin liquids may be found in effective low-energy Hamiltonians, which are based upon the so-called quantum dimer models² or strong-coupling expansions.³ Since then, three main directions can be identified to study quantum spin liquids. The first one is the definition of *ad hoc* Hamiltonians that can be exactly solved to have a cartoon picture of the exotic properties expected in generic systems (e.g., topological degeneracy and fractional excitations).^{4,5} The second one is the classification of different spin-liquid states according to hidden symmetries (i.e., beyond the Ginzburg-Landau description); examples may be given by the projective-symmetry group,⁶ tensor states,⁷ or cohomology.^{8–10} Finally, the third and more pragmatic one is to perform numerical simulations on Heisenberg or Hubbard models, in order to gain evidence that stable spin-liquid phases may indeed exist.^{11–16}

In this Letter, we take the latter point of view and investigate the J_1 – J_2 spin-half Heisenberg model on the two-dimensional square lattice by systematically improving accurate variational wave functions, to obtain a reliable estimate of the *exact* ground state, along with few relevant low-energy states. This procedure allows us to extract the spin gap and show that a gapless spin-liquid phase exists in the highly frustrated regime.

The Heisenberg J_1 – J_2 model is defined by:

$$\mathcal{H} = J_1 \sum_{\langle i,j \rangle} \mathbf{S}_i \cdot \mathbf{S}_j + J_2 \sum_{\langle\langle i,j \rangle\rangle} \mathbf{S}_i \cdot \mathbf{S}_j, \quad (1)$$

where $\mathbf{S}_i = (S_i^x, S_i^y, S_i^z)$ is the quantum spin operator on the site i ; $\langle \dots \rangle$ and $\langle\langle \dots \rangle\rangle$ indicate nearest-neighbor and next-nearest-neighbor sites. Here, we focus on the case where both super-exchange couplings are antiferromagnetic and consider clusters with $N = L \times L$ sites and periodic boundary conditions.

In the unfrustrated case with $J_2 = 0$, it is well established that the ground state has Néel long-range order, with a staggered magnetization that is reduced from its classical value, i.e., $M \simeq 0.307$.^{17,18} For large values of J_2 , the ground state shows again a collinear magnetic order with pitch vector $Q = (\pi, 0)$ or $(0, \pi)$. The intermediate regime, around the strongest frustration point $J_2/J_1 = 0.5$, is the most debated one, since the combined effect of frustration and quantum fluctuations destroys antiferromagnetism and leads to a non-magnetic ground state. However, the nature of this quantum phase is still controversial. Since the pioneering works,^{19–22} it was clear that the problem was terribly complicated: many states can be constructed with very similar energies but very different physical properties, e.g., having dimer or plaquette valence-bond order, or being totally disordered with short- or long-range resonating-valence bond fluctuations. This is mainly due to the fact that the non-magnetic region of the J_1 – J_2 model is relatively small and several generalized susceptibilities may be quite large,²³ indicating that the ground state is on the verge of various instabilities. In this context, there is a convincing evidence that a third-nearest-neighbor coupling J_3 may drive the system into a valence-bond solid.²⁴

Recent density-matrix renormalization group (DMRG) results sparked the desire of understanding the phase diagram of the J_1 – J_2 model, suggesting the existence of a true spin-liquid phase.¹³ In particular, by considering cylindrical geometry, results for the singlet and triplet gaps provided some evidence for a fully gapped Z_2 state in the region $0.41 \leq J_2/J_1 \leq 0.62$, without local broken symmetry. Moreover, the calculation of the so-called topological entanglement entropy γ was found

to be consistent with the expected value of $\gamma = \ln(2)$ for a gapped Z_2 spin liquid. The most natural description of a fully gapped state is given in terms of the Schwinger boson representation of the spin operators.²⁵ By performing a full optimization of the many-body wave function on small sizes, we showed that this kind of bosonic ansatz may qualitatively reproduce some of the DMRG results.²⁶ However, while in the weakly-frustrated regime the bosonic ansatz has magnetic order and excellent variational energy, for $0.45 \lesssim J_2/J_1 \lesssim 0.6$ a state constructed with Abrikosov fermions instead of Schwinger boson has better accuracy.²⁶ In fact, in a forerunner paper,¹¹ three of us showed that, within this kind of fermionic representation, it is possible to have a particularly accurate description of the ground state in the strongly frustrated regime. By using the language of the projective-symmetry group (PSG),⁶ our variational wave function (dubbed Z2Azz13 in Ref. 6) has a Z_2 gauge structure (implying gapped gauge excitations) but gapless spinon excitations with four Dirac points. A gapless spin liquid with topological degeneracy has been also suggested by using projected-entangled pair states on cylindrical geometry.²⁷ These results suggest that a gapless spin liquid may be competitive with the one proposed by DMRG calculations.

In this Letter, we present numerical calculations based upon a systematic improvement of the fermionic Z2Azz13 wave function that allow us to extract (i) the ground state energy, (ii) the energy of the lowest $S = 2$ state, and (iii) the energy of a state with $S = 1$ and $k = (\pi, 0)$ [or $(0, \pi)$], so to extract the information about the *exact* spin gap. The state with $S = 1$ and $k = (\pi, 0)$ is particularly interesting, since it is certainly gapped in the Néel phase and it is not expected to play any important role in a gapped non-magnetic regime (while it is one of the gapless modes in the collinear magnetic phase that appears for large J_2 values). On the contrary, this state is gapless in the Z2Azz13 ansatz (see below for the details). One of the main results of this work is to show that this $S = 1$ excitation becomes indeed gapless in a region around $J_2/J_1 = 0.5$, and, therefore, a spin liquid with gapless triplet excitations both at $k = (\pi, 0)$ and (π, π) represents the most natural candidate between the two magnetic phases characterizing the small and large J_2/J_1 regimes.

Numerical method – The starting variational wave functions are defined through the mean-field Hamiltonian for the Abrikosov-fermion representation of the spin operators:²⁸

$$\begin{aligned} \mathcal{H}_{MF} = & \sum_{i,j,\sigma} t_{i,j} c_{i,\sigma}^\dagger c_{j,\sigma} + h.c. \\ & + \sum_{i,j} \eta_{i,j} (c_{i,\uparrow}^\dagger c_{j,\downarrow}^\dagger + c_{j,\uparrow}^\dagger c_{i,\downarrow}^\dagger) + h.c., \end{aligned} \quad (2)$$

where for each bond (i, j) there are hopping ($t_{i,j}$) and/or pairing ($\eta_{i,j}$) terms; the mean-field Hamiltonian may also contain on-site terms (i.e., chemical potential and/or on-

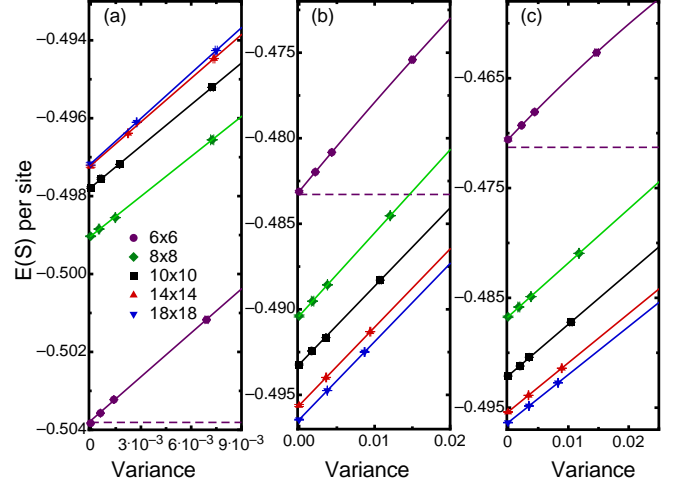


FIG. 1: (Color on-line) Energies per site for the $S = 0$ ground state (a), the $S = 1$ state with $k = (\pi, 0)$ (b), and the $S = 2$ with $k = (0, 0)$ (c) versus the variance for $J_2/J_1 = 0.5$. The results with $p = 0, 1$, and 2 are reported for $L = 6, 8$, and 10 , and with only $p = 0$ and $p = 1$ for $L = 14$ and $L = 18$. The variance extrapolated results are also shown.

site pairing). Given any eigenstate $|\Psi_{MF}\rangle$ of the mean-field Hamiltonian, a physical state for the spin model can be obtained by a projection of it onto the subspace with one fermion per site:

$$|\Psi_v\rangle = \mathcal{P}_G |\Psi_{MF}\rangle, \quad (3)$$

where $\mathcal{P}_G = \prod_i (n_{i,\uparrow} - n_{i,\downarrow})^2$ is the Gutzwiller projector, $n_{i,\sigma} = c_{i,\sigma}^\dagger c_{i,\sigma}$ being the local density. Depending on the symmetry of the mean-field ansatz (e.g., the pattern of the $t_{i,j}$'s and the $\eta_{i,j}$'s), the projected state may describe *different* spin liquids, having for example $U(1)$ or Z_2 gauge structure and gapped or gapless spinon spectrum.⁶

Here, we will consider a state that is obtained by taking a real pairing η_{xy} (with d_{xy} symmetry) on top of the $U(1)$ state with nearest-neighbor hopping t and real pairing $\eta_{x^2-y^2}$ (with $d_{x^2-y^2}$ symmetry). The d_{xy} term is crucial to break the $U(1)$ gauge symmetry down to Z_2 . Restricting this coupling along the $(\pm 2, \pm 2)$ bonds implies *commensurate* Dirac points at $k = (\pm\pi/2, \pm\pi/2)$ in the mean-field spectrum; with this choice, the optimal variational state is found by projecting the ground state of \mathcal{H}_{MF} .²⁹

Besides the ansatz for the ground state, within this formalism, it is straightforward to have simple representations also for excited states. In this respect, it is useful to consider a particle-hole transformation for the down electrons on the mean-field Hamiltonian (2), i.e., $c_{i,\downarrow}^\dagger \rightarrow c_{i,\downarrow}$, such that the transformed Hamiltonian conserves the total number of particles. Then, the ground state is obtained by filling the lowest N orbitals, with suitable boundary conditions (either periodic or anti-periodic) in order to have a unique mean-field ground state. Spin

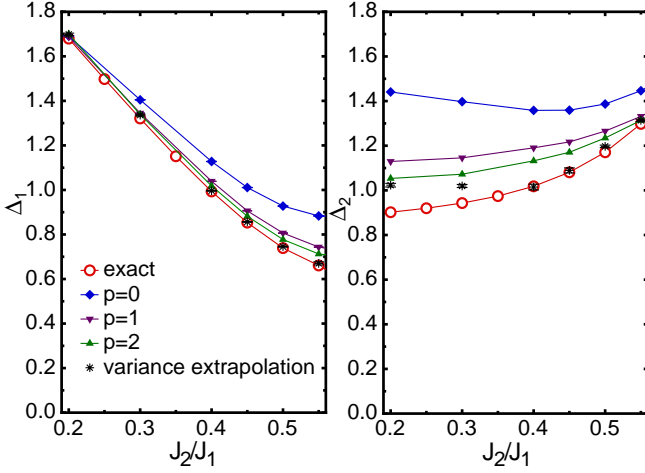


FIG. 2: (Color on-line) Spin gap for the $S = 1$ excitation at $k = (\pi, 0)$ (left panel) and the $S = 2$ excitation with $k = (0, 0)$ (right panel) for the 6×6 cluster. Results for $p = 0, 1$, and 2 Lanczos steps are reported, together with the extrapolated and the exact ones.

excitations can be obtained by creating the appropriate Bogoliubov quasi-particles (spinons) and possibly switching boundary condition. By limiting to states that can be constructed from a single determinant, here we consider a $S = 2$ state with momentum $k = (0, 0)$ and a $S = 1$ state with $k = (\pi, 0)$ or $(0, \pi)$. By performing Monte Carlo calculations, we are able to compute separately the energies of these three states, so to assess the spin gap of the $J_1 - J_2$ model.

In order to systematically improve the variational wave functions, we can apply a number p of Lanczos steps:

$$|\Psi_p\rangle = \left(1 + \sum_{m=1}^p \alpha_m \mathcal{H}^m\right) |\Psi_v\rangle, \quad (4)$$

where α_m are p additional variational parameters. Clearly, whenever $|\Psi_v\rangle$ is not orthogonal to the exact ground state, $|\Psi_p\rangle$ converges to it for large p . Unfortunately, on large sizes, only few steps can be efficiently afforded: here, we consider the case with $p = 1$ and $p = 2$ ($p = 0$ corresponds to the original variational wave function).³⁰ Furthermore, an estimate of the exact energy may be obtained by the variance extrapolation. Indeed, for a systematically convergent sequence of states $|\Psi_p\rangle$ with energy E_p and variance σ_p^2 , it is easy to prove that $E_p \approx E_{\text{ex}} + \text{const} \times \sigma_p^2$, where $E_p = \langle \Psi_p | \mathcal{H} | \Psi_p \rangle / N$ and $\sigma_p^2 = (\langle \Psi_p | \mathcal{H}^2 | \Psi_p \rangle - \langle \Psi_p | \mathcal{H} | \Psi_p \rangle^2) / N$ are the energy and variance per site, respectively. Therefore, the exact energy E_{ex} may be extracted by fitting E_p vs σ_p^2 , for $p = 0, 1$, and 2.

Results – A systematic analysis shows that the best possible ansatz for the variational wave function of the form (3) has a non-vanishing d_{xy} pairing in the whole regime $0.45 \lesssim J_2/J_1 \lesssim 0.6$. Here, both the static structure factor $S(q)$ and the dimer-dimer correlations

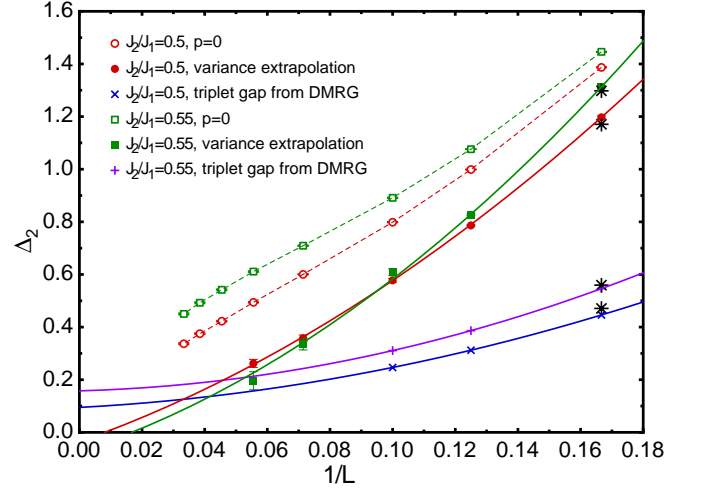


FIG. 3: (Color on-line) The $S = 2$ spin gap as a function of the system size for the variational wave function and the Lanczos extrapolation for two values of J_2 . The thermodynamic extrapolations are consistent with a vanishing gap within the error bars, i.e., $\Delta_2 = -0.04(5)$ and $-0.07(7)$ for $J_2/J_1 = 0.5$ and 0.55 , respectively. The DMRG results on $2L \times L$ cylinders (with open boundary conditions along x and periodic along y) for the $S = 1$ excitation are also shown.¹³ Exact results (stars) of the $S = 2$ gap and the lowest $S = 1$ gap on the 6×6 cluster (with periodic boundary conditions) are reported.

do not show any evidence for the occurrence of ordered states,^{11,31} in agreement with the DMRG results of Ref. 13.

Let us start by showing the accuracy of our method for the ground state and the two excitations: $S = 1$ at $k = (\pi, 0)$ and $S = 2$ at $k = (0, 0)$. In Fig. 1, we report calculations for $J_2/J_1 = 0.5$ and different sizes of the cluster. For $L = 6$, where the exact results can be obtained by Lanczos diagonalizations, our extrapolations are extremely accurate. Moreover, for the ground state, our best variational $p = 2$ state gives $E/J_1 = -0.503571(3)$, while $E_{\text{ex}}/J_1 = -0.50381$; remarkably, the Lanczos step procedure remains effective even for larger sizes, the difference between the best variational state with $p = 2$ and the extrapolated being very weakly size dependent (for $L = 10$, the $p = 2$ energy is $E/J_1 = -0.497549(2)$, while the extrapolated one is $E/J_1 = -0.49781(2)$). The same applies also for excited states, see Fig. 1. The almost perfect alignment of the Lanczos steps, together with the impressive accuracy obtained up to relatively large clusters, clearly indicates that the exact ground state should be essentially described by the starting Z_2 gapless state.

In Fig. 2, we show the results for the $S = 1$ spin gap Δ_1 at $k = (\pi, 0)$ and the $S = 2$ spin gap Δ_2 for the 6×6 cluster, in comparison with the exact results. Remarkably, our approach based upon a spin-liquid wave function gives excellent accuracy on Δ_1 in the whole region $0.2 \leq J_2/J_1 \leq 0.55$. A similar accuracy is also obtained for Δ_2 in the strongly frustrated region (i.e., $0.4 \leq J_2/J_1 \leq 0.55$) even though this is not a sim-

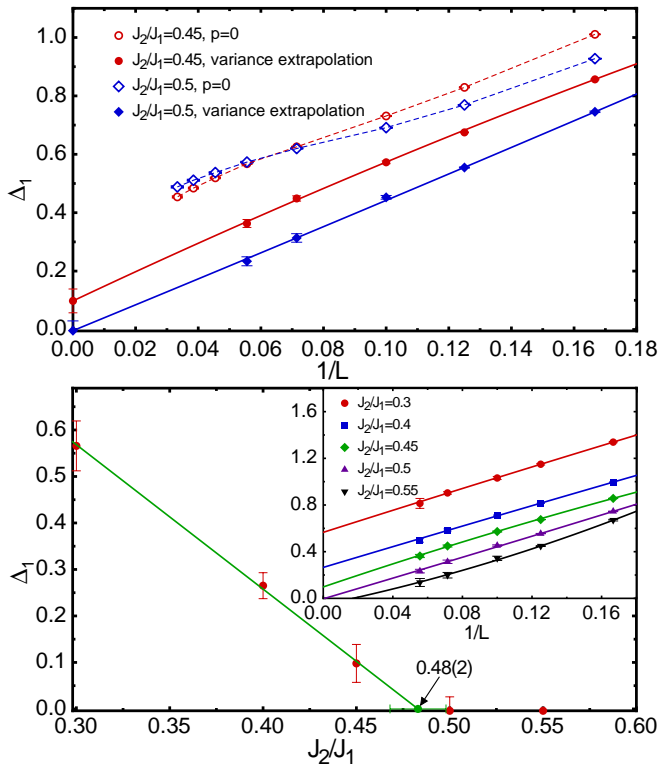


FIG. 4: (Color on-line) The $S = 1$ with $k = (\pi, 0)$ spin gap as a function of the system size for the variational wave function and the Lanczos extrapolation for two values of J_2 (upper panel). The behavior of the extrapolated gap as a function of J_2/J_1 is reported in the lower panel, the line is a guide to the eye. The Lanczos extrapolated gap as a function of L for different values of J_2 are also reported in the inset.

ple excitation since it involves four spinons. Instead, at $J_2/J_1 \simeq 0.6$ the accuracy deteriorates because a first-order transition to the collinear magnetic state takes place in the thermodynamic limit;^{13,19,32} in this region, a quasi-degeneracy of levels in the energy spectrum occurs, leading to a reduced overlap between the variational wave function and the lowest exact eigenstate.^{11,31}

Then, we consider larger cluster and perform a size scaling of the gaps, see Figs. 3 and 4 for the $S = 2$ and $S = 1$ with $k = (\pi, 0)$, respectively. For $L \geq 6$, the extrapolations obtained with two ($p = 0$ and 1) or three ($p = 0, 1$, and 2) points are perfectly consistent (i.e., the three points lie along a straight line, see Fig. 1). Therefore, we perform the computationally demanding second Lanczos step only for relatively small clusters (up to the $L = 10$), while we limit to the first Lanczos step for large clusters (up to the $L = 18$).

The $S = 2$ gap is reported for two values of the frustrating ratio J_2/J_1 , together with the $S = 1$ gap obtained by DMRG calculations of Ref. 13. We find that the Lanczos step procedure clearly reduces the gap on any size. In contrast with the DMRG picture, we have a clear evidence that the spin gap closes when $L \rightarrow \infty$ for $J_2/J_1 = 0.5$ and 0.55. Indeed, the values that we

obtain in the thermodynamic limit are both compatible with a vanishing gap, i.e., $\Delta_2 = -0.04(5)$ and $-0.07(7)$, see Fig. 3. We want to stress that our calculations are done on square clusters, having all the symmetries of the infinite lattice, and periodic boundary conditions, while DMRG calculations employed cylinders with $2L \times L$ sites and open boundary conditions along x . A possible explanation for having a finite gap within DMRG is that this method favors low-entangled states with finite gaps. On the contrary, our variational approach is more flexible, allowing both gapped and gapless states. At the pure $p = 0$ variational level, the best wave function of the form (3) is found to be gapless, its energy being the lowest one among all states constructed from Schwinger bosons and Abrikosov fermions for $0.45 \lesssim J_2/J_1 \lesssim 0.6$;²⁶ moreover, by applying few Lanczos steps, the finite-size gap lowers with no evidence for a finite value in the thermodynamic limit.

Finally, the $S = 1$ gap with $k = (\pi, 0)$ has been computed for various values of J_2 and cluster sizes, see Fig. 4. This gap is finite in the Néel phase for small J_2/J_1 , where the only gapless $S = 1$ excitations have $k = (0, 0)$ and $k = (\pi, \pi)$. Indeed, this is what is found for $J_2/J_1 \lesssim 0.48$ when the Lanczos extrapolation is considered, even if the starting variational wave function is gapless before Gutzwiller projection. Remarkably, in agreement with the theoretical picture of the Z2Azz13 spin liquid, this gap vanishes for the two cases we investigated within the spin liquid region: $J_2/J_1 = 0.5$ and 0.55 (before the transition to the collinear magnetic phase, which occurs for $J_2/J_1 \gtrsim 0.6$). We expect that the $S = 1$ gap at $k = (\pi, 0)$ closes for $J_2 \rightarrow J_2^c$ with a non-trivial exponent smaller than one, which is however not possible to estimate with our numerical results. Nevertheless, by performing a linear fit of our data, we can obtain an upper bound of the Néel to spin liquid transition, which can be located at $J_2^c = 0.48(2)$.

Conclusions – In conclusion, by using a particularly accurate variational state and a procedure based upon the application of few Lanczos steps, we showed that it is possible to extract important information on the spin gap of frustrated spin models. In particular, we provided a solid evidence that the spin-liquid phase of the $J_1 - J_2$ model on the square lattice is gapless and may be very well described by using a Abrikosov-fermion mean field with a Z_2 gauge structure and gapless spinons with four Dirac points at $k = (\pm\pi/2, \pm\pi/2)$. The latter statement is further supported by the occurrence of a vanishing $S = 1$ gap at the non-trivial momenta $k = (\pi, 0)$ and $(0, \pi)$. Our calculations give the first direct evidence for the existence and the stability of highly-entangled gapless spin liquids in $SU(2)$ spin models.

We thank Y. Iqbal and S.L. Sondhi for useful discussions. F.B. thanks P.A. Lee and H.-C. Jiang for very interesting discussions during the KITP program “Frustrated Magnetism and Quantum Spin Liquids: From Theory and Models to Experiments” and partial support from the National Science Foundation under the Grant

No. NSF PHY11-25915. We acknowledge support from PRIN 2010-11.

-
- ¹ L. Balents, *Nature* **464**, 199 (2010).
 - ² R. Moessner and S. Sondhi, *Phys. Rev. Lett.* **86**, 1881 (2001).
 - ³ L. Balents, M.P.A. Fisher, and S.M. Girvin, *Phys. Rev. B* **65**, 224412 (2002).
 - ⁴ A.Y. Kitaev, *Ann. Phys.* **303**, 2 (2003).
 - ⁵ A.Y. Kitaev, *Ann. Phys.* **321**, 2 (2005).
 - ⁶ X.-G. Wen, *Phys. Rev. B* **65**, 165113 (2002).
 - ⁷ X. Chen, Z.-C. Gu, and X.-G. Wen, *Phys. Rev. B* **83**, 035107 (2011); N. Schuch, D. Perez-Garcia, and I. Cirac, *Phys. Rev. B* **84**, 165139 (2011).
 - ⁸ X. Chen, Z.-C. Gu, Z.-X. Liu, and X.-G. Wen, *Phys. Rev. B* **87**, 155114 (2013).
 - ⁹ A.M. Essin and M. Hermele, *Phys. Rev. B* **87**, 104406 (2013).
 - ¹⁰ A. Mesaros and Y. Ran, *Phys. Rev. B* **87**, 155115 (2013).
 - ¹¹ L. Capriotti, F. Becca, A. Parola, and S. Sorella, *Phys. Rev. Lett.* **87**, 097201 (2001).
 - ¹² S. Yan, D. Huse, and S. White, *Science* **332**, 1173 (2011).
 - ¹³ H.-C. Jiang, H. Yao, and L. Balents, *Phys. Rev. B* **86**, 024424 (2012).
 - ¹⁴ Y. Iqbal, F. Becca, S. Sorella, and D. Poilblanc, *Phys. Rev. B* **87**, 060405 (2013).
 - ¹⁵ Z.Y. Meng, T.C. Lang, S. Wessel, F.F. Assaad, and A. Muramatsu, *Nature* **464**, 847 (2010).
 - ¹⁶ S. Sorella, Y. Otsuka, and S. Yunoki, *Sci. Rep.* **2**, 992 (2012).
 - ¹⁷ A.W. Sandvik, *Phys. Rev. B* **56**, 11678 (1997).
 - ¹⁸ M. Calandra Buonaurea and S. Sorella, *Phys. Rev. B* **57**, 11446 (1998).
 - ¹⁹ P. Chandra and B. Doucot, *Phys. Rev. B* **38**, 9335 (1988).
 - ²⁰ N. Read and S. Sachdev, *Phys. Rev. Lett.* **62**, 1694 (1989).
 - ²¹ M.P. Gelfand, R.R.P. Singh, and D.A. Huse, *Phys. Rev. B* **40**, 10801 (1989).
 - ²² F. Figueirido, A. Karlhede, S. Kivelson, S. Sondhi, M. Rocek, and D.S. Rokhsar, *Phys. Rev. B* **41**, 4619 (1990).
 - ²³ R. Darradi, O. Derzhko, R. Zinke, J. Schulenburg, S.E. Kruger, and J. Richter, *Phys. Rev. B* **78**, 214415 (2008).
 - ²⁴ M. Mambrini, A. Lauchli, D. Poilblanc, and F. Mila, *Phys. Rev. B* **74**, 144422 (2006).
 - ²⁵ D.P. Arovas and A. Auerbach, *Phys. Rev. B* **38**, 316 (1988).
 - ²⁶ T. Li, F. Becca, W.-J. Hu, and S. Sorella, *Phys. Rev. B* **86**, 075111 (2012).
 - ²⁷ L. Wang, D. Poilblanc, Z.-C. Gu, X.-G. Wen, and F. Verstraete, *arXiv:1301.4492*.
 - ²⁸ G. Baskaran, Z. Zou, and P.W. Anderson, *Solid State Commun.* **63**, 973 (1987); G. Baskaran and P.W. Anderson, *Phys. Rev. B* **37**, 580 (1988).
 - ²⁹ In this approach, all pairing terms are variational parameters that can be optimized in order to lower the total energy by using the method described by S. Sorella, *Phys. Rev. B* **71**, 241103 (2005). For $L > 6$, we considered $\eta_{x^2-y^2}$ terms for bonds (1,0), (2,1), and (3,0) (and symmetry related ones) and η_{xy} terms for $(\pm 2, \pm 2)$ bonds.
 - ³⁰ Within quantum Monte Carlo calculations, in order to have a stable and accurate algorithm for p Lanczos steps, it is important to adopt a suitable regularization scheme to avoid vanishingly small determinants. Here, we considered to sample configurations $|x\rangle$ such that: $\langle x|\mathcal{H}|\Psi_v\rangle/\langle x|\Psi_v\rangle > N/\epsilon$, with $\epsilon = 10^{-6}$ (no appreciable change is found with ϵ ranging from 10^{-8} to 10^{-4}); W.-J. Hu, F. Becca, A. Parola, and S. Sorella, in preparation.
 - ³¹ F. Becca, L. Capriotti, A. Parola, and S. Sorella, *Springer Ser. Solid-State Sci.* **164**, 379 (2011).
 - ³² H.J. Schulz, T. Ziman, and D. Poilblanc, *J. Phys. I* **6**, 675 (1996).

TABLE I: p=0

	$J_2/J_1 = 0.4$	$J_2/J_1 = 0.45$	$J_2/J_1 = 0.5$	$J_2/J_1 = 0.55$
$L = 6$ $S = 0$	-0.52715(1)	-0.51364(1)	-0.50117(1)	-0.48992(1)
$S = 1$	-0.49582(1)	-0.48557(1)	-0.47541(1)	-0.46538(2)
$S = 2$			-0.46265(2)	-0.44974(2)
$L = 8$ $S = 0$	-0.52302(1)	-0.50930(1)	-0.49656(1)	-0.48487(1)
$S = 1$	-0.50835(1)	-0.49635(1)	-0.48453(1)	-0.47299(1)
$S = 2$			-0.48095(1)	-0.46806(1)
$L = 10$ $S = 0$	-0.52188(1)	-0.50811(1)	-0.49521(1)	-0.48335(1)
$S = 1$	-0.51362(1)	-0.50080(1)	-0.48830(1)	-0.47625(1)
$S = 2$			-0.48722(1)	-0.47443(1)
$L = 14$ $S = 0$	-0.52124(1)	-0.50745(1)	-0.49447(1)	-0.48242(1)
$S = 1$	-0.51772(1)	-0.50425(1)	-0.49131(1)	-0.47904(1)
$S = 2$			-0.49141(1)	-0.47880(1)
$L = 18$ $S = 0$	-0.52107(1)	-0.50728(1)	-0.49426(1)	-0.48215(1)
$S = 1$	-0.51921(1)	-0.50553(1)	-0.49249(1)	-0.48018(1)
$S = 2$			-0.49274(1)	-0.48026(1)

TABLE II: p=1

	$J_2/J_1 = 0.4$	$J_2/J_1 = 0.45$	$J_2/J_1 = 0.5$	$J_2/J_1 = 0.55$
$L = 6$ $S = 0$	-0.52928(1)	-0.51538(1)	-0.50323(1)	-0.49303(1)
$S = 1$	-0.50042(1)	-0.49020(1)	-0.48082(1)	-0.47238(1)
$S = 2$			-0.46807(1)	-0.45605(1)
$L = 8$ $S = 0$	-0.52501(1)	-0.51101(1)	-0.49855(1)	-0.48777(1)
$S = 1$	-0.51157(1)	-0.49963(1)	-0.48857(1)	-0.47847(1)
$S = 2$			-0.48489(1)	-0.47305(1)
$L = 10$ $S = 0$	-0.52368(1)	-0.50973(1)	-0.49718(1)	-0.48622(1)
$S = 1$	-0.51610(1)	-0.50344(1)	-0.49165(1)	-0.48090(1)
$S = 2$			-0.49041(1)	-0.47867(1)
$L = 14$ $S = 0$	-0.52287(1)	-0.50899(1)	-0.49638(1)	-0.48519(1)
$S = 1$	-0.51966(1)	-0.50632(1)	-0.49398(1)	-0.48270(1)
$S = 2$			-0.49387(1)	-0.48221(1)
$L = 18$ $S = 0$	-0.52259(1)	-0.50874(1)	-0.49611(1)	-0.48475(1)
$S = 1$	-0.52083(5)	-0.50137(1)	-0.49475(1)	-0.48327(1)
$S = 2$			-0.49485(1)	-0.48319(1)

TABLE III: p=2

	$J_2/J_1 = 0.4$	$J_2/J_1 = 0.45$	$J_2/J_1 = 0.5$	$J_2/J_1 = 0.55$
$L = 6$ $S = 0$	-0.52957(1)	-0.51558(1)	-0.50357(1)	-0.49399(1)
$S = 1$	-0.50130(1)	-0.49108(1)	-0.48197(1)	-0.47419(1)
$S = 2$			-0.46929(1)	-0.45750(1)
$L = 8$ $S = 0$	-0.52539(1)	-0.51125(1)	-0.49886(1)	-0.48841(2)
$S = 1$	-0.51224(2)	-0.50033(1)	-0.48952(1)	-0.48008(4)
$S = 2$			-0.48583(4)	-0.47443(2)
$L = 10$ $S = 0$	-0.5240(1)	-0.51001(1)	-0.49755(1)	-0.48693(3)
$S = 1$	-0.51671(7)	-0.50398(1)	-0.49243(1)	-0.4825(2)
$S = 2$			-0.49121(3)	-0.4800(2)
$L = 14$ $S = 0$				
$S = 1$				
$S = 2$				
$L = 18$ $S = 0$				
$S = 1$				
$S = 2$				

TABLE IV: extrapolation

	$J_2/J_1 = 0.4$	$J_2/J_1 = 0.45$	$J_2/J_1 = 0.5$	$J_2/J_1 = 0.55$
$L = 6$ $S = 0$	-0.52972(1)	-0.51566(1)	-0.50382(1)	-0.49521(7)
$S = 1$	-0.50204(5)	-0.49187(4)	-0.48312(6)	-0.4766(1)
$S = 2$			-0.4706(1)	-0.4587(1)
$L = 8$ $S = 0$	-0.52556(1)	-0.51140(1)	-0.49906(1)	-0.48894(3)
$S = 1$	-0.51282(1)	-0.50085(1)	-0.49039(2)	-0.48194(3)
$S = 2$			-0.48677(1)	-0.47602(3)
$L = 10$ $S = 0$	-0.52429(2)	-0.51017(2)	-0.49781(2)	-0.48766(6)
$S = 1$	-0.51718(3)	-0.50445(3)	-0.49329(5)	-0.4842(1)
$S = 2$			-0.49203(5)	-0.48157(8)
$L = 14$ $S = 0$	-0.52351(2)	-0.50953(1)	-0.49722(2)	-0.48696(5)
$S = 1$	-0.52052(2)	-0.50724(3)	-0.49562(5)	-0.48594(7)
$S = 2$			-0.49539(4)	-0.48524(9)
$L = 18$ $S = 0$	-0.52333(1)	-0.50940(1)	-0.49717(2)	-0.48698(5)
$S = 1$	-0.52180(4)	-0.50828(3)	-0.49645(3)	-0.48656(5)
$S = 2$			-0.49636(3)	-0.48638(5)